

## The Wing Beat of *Drosophila Melanogaster*. III. Control

J. M. Zanker

*Phil. Trans. R. Soc. Lond. B* 1990 **327**, 45-64  
doi: 10.1098/rstb.1990.0042

### References

Article cited in:

<http://rstb.royalsocietypublishing.org/content/327/1238/45#related-urls>

### Email alerting service

Receive free email alerts when new articles cite this article - sign up in the box at the top right-hand corner of the article or click [here](#)

To subscribe to *Phil. Trans. R. Soc. Lond. B* go to: <http://rstb.royalsocietypublishing.org/subscriptions>

# THE WING BEAT OF *DROSOPHILA MELANOGASTER*

## III. CONTROL

By J. M. ZANKER

Max-Planck-Institut für biologische Kybernetik, Spemannstrasse 38, D-7400 Tübingen, F.R.G.

(Communicated by M. F. Land, F.R.S. – Received 26 August 1988)

### CONTENTS

	PAGE
1. INTRODUCTION	46
2. MATERIALS AND METHODS	48
(a) Kinematic analysis	48
(b) Aerodynamic analysis	49
(c) Wind stimuli	49
(d) Visual stimuli	49
3. RESULTS AND DISCUSSION	50
(a) Response to wind stimuli	50
(b) Response to visual stimuli	56
4. CONCLUSIONS	62
REFERENCES	63

Two major problems have to be solved by a flying animal or machine. (i) On the time average, flight force has to be *produced* which is sufficient to keep the body airborne and to propel it through the air. (ii) To stabilize a given position or trajectory, the vector of the generated flight force has to be *controlled* in its magnitude, orientation and position relative to the body. In the present study, the response of wing-beat kinematics to wind and visual stimuli was investigated in tethered flying *Drosophila melanogaster*. When the fly is subjected to an air stream in a wind tunnel, or to striped patterns moving in its frontal field of view, the overall shape of the wing path is altered, including variations of the wing-beat amplitude and the angles of attack. The aerodynamic forces were calculated from the kinematic data according to the quasi-steady aerodynamic theory, to investigate whether this approach is sufficient to describe the control mechanisms of the fly. The stimulus-induced changes of kinematic and aerodynamic variables were compared with control reactions expected in free flight or measured during tethered flight under similar stimulus conditions. In general, the calculated flight forces are too small to account for the measured lift, thrust and torque responses to the particular stimuli, or would even increase the input stimulus instead of being compensatory. This result supports the notion that unsteady aerodynamic mechanisms are likely to play the major role in flapping flight. Following this line of thought, some kinematic responses can be qualitatively understood in terms of unsteady aerofoil action.

## 1. INTRODUCTION

Any flying animal or machine has to solve two basic problems. (i) Sufficient flight force has to be produced to lift the flying object from the ground (i.e. to overcome gravitational forces) and to propel it through the air (i.e. to counteract frictional forces). For a long time, the analysis of animal flight was centred around the question of how these flight forces are generated. The hovering flight of small insects attracted particular interest because in this situation effective force production appears to be incompatible with conventional aerofoil action (for a comprehensive review, see Ellington (1984 *a-f*)). Some aspects of the kinematics and dynamics of tethered flight of *Drosophila melanogaster* were discussed in the two previous papers (Zanker 1990; Zanker & Götz 1990). (ii) To keep a certain flight trajectory or to hover on the spot, the magnitude and the direction of the average flight-force vector, as well as the position of this vector relative to the centre of gravity, have to be controlled. Such control operations enable a fly to gain height, speed up, or turn about some body axis. Visually induced changes of the wing-beat amplitudes and the corresponding torque were investigated thoroughly in tethered flying flies and interpreted as means of course stabilization (see, for example, Götz 1968, 1983). So far, however, only gross changes in motor action have been considered and comparatively simple models of the control system have been developed. It seems worth while to take a closer look at this problem, because flight-force generation and control must depend on each other, leading to an expectedly high level of coadaptation of biological flight motors and sensory and information-processing systems. Thus any progress in the understanding of one of these two aspects of animal flight should help us to understand the other aspect. This complementation is illustrated in this paper by investigation of the kinematics and aerodynamics of control responses induced by external stimulation of tethered flying *Drosophila melanogaster*. Despite the bulk of evidence concerning flight control of bigger insects (Dugard 1967; Zarnack & Möhl 1977; Baker 1979; Pfau & Nachtigall 1981; Alexander 1986; Zarnack 1988, for instance), the discussion is here restricted to dipterans, mainly because a flight control system based on only two wings appears to be less complicated to understand.

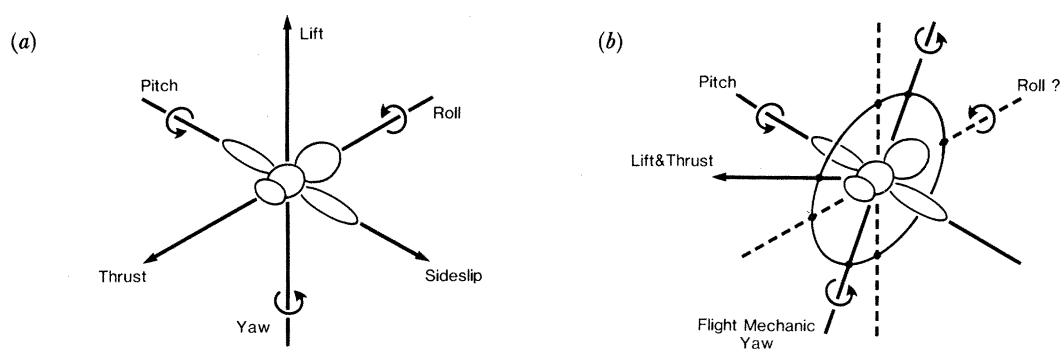


FIGURE 1. Degrees of freedom of flight. (a) When an animal is free to move in space, it may rotate independently about the three body axes (yaw, pitch, roll) and may translate independently along each of these axes (lift, sideslip, thrust). (b) Gross changes of the motor output of *Drosophila melanogaster* during tethered flight in still air can be related to a reduced flight control system. Torque about the yaw axis of flight mechanics is controlled by the *difference* between the wing-beat amplitudes of the two wings, and the lateral abdomen deflection. Lift and thrust are determined by the *sum* of the wing-beat amplitudes of both wings. The ratio between lift and thrust is controlled together with the body pitch by a translatory shifting of the average wing-stroke plane and dorsoventral abdomen deflections.

As sketched in figure 1 *a*, an object flying in space is generally able to translate independently along three directions (i.e. to generate independent thrust, lift and sideslip components of flight force), and to rotate independently about three axes (i.e. to generate independent roll, yaw and pitch torque components). How many of these six degrees of freedom are actually controlled depends on the specific construction of a particular flying machine or animal, which is expected to be adapted to the physical or biological demands on that system. External bursts of wind or internal irregularities of the motor system may induce deviations from a given flight trajectory. To compensate for such perturbations, a feedback control of the flight motor output is required, which may rely on various sensory inputs. One approach to investigate the flight control of flying insects is to elicit control responses by simulating disturbances. In the present context, the influence of two sensory systems was investigated: the mechanosensory response to wind stimuli, and the visual response to large-field pattern motion.

By reduction of the degrees of freedom, a simple flight control system has been proposed for *Drosophila melanogaster* (Vogel 1967; Götz 1968; Götz *et al.* 1979; David 1985; Zanker 1988 *a*, *b*) which accounts for visual course, height and speed stabilization. Basically, the fly is treated like a helicopter with two rotors (left and right wing), each producing an independent average flight-force vector which can be varied in its magnitude by variation of the particular wing-stroke area (wing-beat amplitude). The orientation of these vectors relative to the fly's body is constant because they are expected perpendicular to the average stroke plane, which appears to be inclined with a constant angle relative to the body. Differences between the left and right wing-beat amplitudes, and lateral deflections of the abdomen, lead to torques about the 'yaw axis of flight mechanics', which is tilted 30° backwards relative to the vertical body axis (Zanker 1988 *a*). The overall magnitude of flight force – i.e. both the lift and the thrust component – is determined by the sum of the left and the right wing-beat amplitudes. The ratio between the influence of this vector on height and speed (i.e. between the lift and the thrust component) can only be adjusted to a given control situation by alteration of the body's inclination in space, because of the force vector's fixed orientation relative to the body (Götz & Wandel 1984; David 1978). Such changes in body pitch angle could be generated by dorsoventral abdomen deflections and displacements of the average stroke plane observed in tethered flight (Zanker 1988 *b*), which shift the position of the average flight force vector relative to the fly's centre of gravity. As sketched in figure 1 *b*, five independent motor components (wing-beat amplitudes of left and right wing, position of the average wing stroke plane, lateral and dorsoventral deflections of the abdomen) are combined into a control system which allows for three degrees of freedom of flight (rotation about the yaw axis of flight mechanics, sum of lift and thrust force, body pitch angle determining the ratio between lift and thrust forces). It should be noted that these considerations rely on simplified models of aerodynamics, which might be far from physical reality. Based on the exact kinematics of the wings, in this paper the forces and torques are calculated according to the quasi-steady aerodynamic theory. It will be interesting to know whether this theory, if not sufficient to explain flight force production satisfyingly (see paper 2), is able to describe the control mechanisms adequately, as is assumed implicitly in most of the considerations of flight control.

From the behaviour of freely and tethered flying flies, it is evident that the control system might be more complicated than suggested by the simple control model sketched in figure 1 *b*, and more degrees of freedom are allowed for. (i) At least for short time intervals, in some insects the coupling between the lift:drag ratio and body pitch is relaxed. In *Calliphora*, transient

variations of the ratio between lift and thrust were observed to be independent of body pitch (Blondeau 1981; Nachtigall & Roth 1983). In locusts the independent adjustment of lift and thrust, called 'lift-control reaction', was attributed to the variation of the angles of attack of the wings (Gettrup & Wilson 1964). (ii) The difference between the angles of attack of the right and left wing observed in tethered flying *Calliphora* during roll stimulation (Hengstenberg *et al.* 1986), which accompanies alterations of the average wing-beat amplitude on either side (Srinivasan 1977), possibly indicates an independent control of the fly's roll angle not covered by the simple model so far. (iii) Freely flying hoverflies seem to be able to manoeuvre with all six degrees of freedom. For instance, they are able to move sideways without changing body posture, in addition to the obviously independent generation of lift and thrust (Collett & Land 1975). However, indications of sideslip in freely flying *Musca* could be explained without assuming active sideways force components, solely by inertial and centrifugal forces (Wagner 1986).

The kinematic and aerodynamic analysis introduced in the preceding two papers will serve us as a tool to investigate whether the simple flight control model has to be refined in two aspects. 1. Can prominent variations of the wing-beat *kinematics* be elicited by mechanosensory or visual stimuli and can these effects be attributed to some of the six degrees of freedom of flight? A set of 17 pairs of steering muscles seems to be developed in Diptera of all sizes (Zalokar 1947; Heide 1983), despite the possible reduction of complexity of the flight control system in small flies such as *Drosophila*, which are bound to operate at low Reynolds numbers. At least three pairs of steering muscles have been found to contribute to the control of both course and altitude in *Drosophila* (Götz 1983, 1987*b*) by influencing the difference and the sum of the wing-beat amplitude on either side. Can other steering muscles be associated with possible other kinematic variations discovered so far? 2. Are the *aerodynamic consequences* of the kinematic modifications adequately described by the quasi-steady theory? In the preceding paper (Zanker & Götz 1990) it was concluded that unsteady aerodynamic mechanisms play the major role in flight-force production. Nevertheless, the kinematic data for stimulated flight will be subjected to the quasi-steady calculations, in order to investigate whether this theory (which implicitly has been the basis of most discussions of insect flight control) explains control mechanisms satisfyingly. If this is not possible either, control models have to include unsteady aerodynamic mechanisms, and the kinematic basis of the control mechanisms have to be discussed with regard to these concepts.

## 2. MATERIALS AND METHODS

### (a) *Kinematic analysis*

Kinematic data were acquired as described in paper 1 (Zanker 1990). The postures of the wings were reconstructed in space from 'artificial' slow-motion pictures (taken at a rate of  $1 \text{ s}^{-1}$ ) by digitizing typical points on the wing surface in two different photographic projections of the tethered flying fly. Each wing is represented by a set of three orthogonal axes fitted to the digitized wing coordinates. The time course of the variables is plotted on a 'non-dimensional' timescale, given by fractions of the wing-beat cycle. The same set of data is displayed twice to facilitate the evaluation of the periodic events. The data shown in the present report are the time averages over several wing-beat cycles and the average over several flies. The standard errors of the mean, which were calculated as in paper 2 (Zanker & Götz 1990), are given in the figure legends.

*(b) Aerodynamic analysis*

From the kinematic data the aerodynamic forces were calculated according to the quasi-steady assumption. The procedure of these calculations, as well as the limitations of this approach, were discussed in paper 2; the morphological parameters and the coefficients of lift and drag required for the calculations were derived in the same paper. All aerodynamic forces presented here were calculated according to the 'blade-element-theory' as weighted averages along the wing spread. The calculated force components are given with reference to the body axes coordinate system. This allows us to predict immediately how flight-force changes would affect the flight trajectory of a freely moving fly. It has to be remembered that the quasi-steady calculations are based on rather crude approximations, such as the neglect of any spatial or temporal variation of the induced wind. Therefore, all our estimates of control forces and moments have to be interpreted with caution. Although it is clear that quasi-steady aerodynamics is unlikely to explain all aspects of flapping flight of *Drosophila*, the kinematic data were subjected to these calculations, to test whether the *control mechanisms* could be explained satisfyingly by this approach. By comparison of the calculated forces and moments with measurements under similar stimulus conditions, the relevance of unsteady mechanisms and possible kinematic candidates for such mechanisms could be assessed.

*(c) Wind stimuli*

The experimental setup for 'artificial' slow-motion cinematography (see Zanker 1990) was compact enough to be positioned inside the open section (diameter 0.03 m, length 0.06 m) of a miniature wind tunnel (for a description of the wind tunnel, see Götz (1983)). All sharp edges of the block carrying the mirrors and light guides for the multi-projectional viewing of the fly were rounded to prevent strong turbulence of the air flow. By introducing thin smoke streams, it was crudely verified that the air flow was laminar in the area where the tethered flying fly was positioned during the experiments. Some time before the filming started, the wind speed was set to 1.0 (0.5, 0) m s<sup>-1</sup>. Each test fly was stimulated with various wind speeds in randomized order to reduce the effects of fatigue or other slow time-dependent processes. After selection of the stable flight episodes (cf. paper 1) 806 (411, 754) single frames could be evaluated from  $N = 13$  (7, 14) flies, leading to a mean number of data points per time step of  $n = 64$  (33, 60) for the wind speed of 1 m s<sup>-1</sup>. (The numbers in brackets refer to 0.5 m s<sup>-1</sup> and to still air, respectively.)

*(d) Visual stimuli*

From the centre of the experimental mirror block (see figure 1*a* in paper 1) the fly looked at an oscilloscope monitor (TEKTRONIX 608) positioned in the frontal area of the visual field. Dark and light gratings were displayed on this screen inside a circular aperture of 60° diameter by means of an electronic pattern generator (Innisfree Picasso). The spatial wavelength of the square-wave pattern was 30°; its contrast was about 0.6.

Three stimulus situations were chosen here, which simulate rotations about the three body axes by corresponding pattern motion in the fly's frontal visual field. 1. Stripes moving to the right or to the left in the frontal field of view simulate rotations about the vertical body axis and are called 'yaw' stimuli. It should be noted, however, that these stimuli are ambiguous, because sideslip along the transverse axis will lead to the same type of pattern motion. The gratings were moving at a speed of 30 deg s<sup>-1</sup>, leading to a temporal frequency of 1 Hz. 2. Stripes moving upwards or downwards in the frontal field of view simulate rotations about the

transverse body axis and are called ‘pitch’ stimuli. These stimuli are ambiguous, because translations along the fly’s vertical body axis will cause the same pattern shifts. Again, the pattern speed was  $30 \text{ deg s}^{-1}$ . 3. In contrast, the clockwise or anticlockwise rotations of the frontally presented stripe pattern about the fly’s longitudinal body axis correspond unambiguously to rotations of the fly about this axis and are called ‘roll’ stimuli. The speed of rotation was  $180 \text{ deg s}^{-1}$ , corresponding to 2 s per rotation.

Just like wind stimuli, the visual stimuli were switched on some time before filming commenced, to induce steady flight conditions. Each fly was subjected to the whole set of  $3 \times 2$  stimulus conditions once or twice, with the axes and the signs of the simulated rotations given in randomized order. After selection of the stable flight episodes, 467 single frames could be evaluated from  $N = 11$  flies for the stripes moving to the left. For gratings moving to the right, upwards, downwards, rotating clockwise, and counterclockwise, 518, 486, 472, 428, and 518 single frames were evaluated from 12, 11, 12, 11, and 13 flies, respectively.

### 3. RESULTS AND DISCUSSION

#### (a) *Response to wind stimuli*

When the fly is subjected to head wind in the physiological range between hovering flight ( $0 \text{ m s}^{-1}$ ) and fast forward flight (about  $1 \text{ m s}^{-1}$ ), its wing beat kinematics changes considerably. The two most prominent aspects can already be identified in the wing paths sketched in figure 2. The wing’s trajectories and inclinations are plotted in the left column as top view parallel projection, and in the right column as lateral view ‘football’ projection (for a description of these two projections, see paper 1).

The parallel projection (left column of figure 2) illustrates the changes in wing beat during the dorsal reversal phase, as seen from above. Here, in still air (top row), the wings approach and touch each other starting with their leading edges and then separate, again beginning from the leading edge, like the opening of a flexible book. This so-called ‘squeeze–peel’ was interpreted as means of improving lift production by the exchange of complementary start- and stop-vortices of the two wings (Weis-Fogh 1973; Lighthill 1973; Maxworthy 1981; Ellington 1984*d*). Because in the present reconstruction the wing is represented by a set of three axes, the bending of the wing (which is preserved by the primary reconstruction (see figure 2 of paper 1) cannot be identified in figure 2. However, it can be seen that the two wings touch each other and that they are pronated during the reversal phase. At wind speeds of  $1 \text{ m s}^{-1}$  (bottom row), the wings’ elevation during the dorsal reversal phase is reduced. In consequence, they do not touch each other, i.e. the squeeze–peel is given up and the pronation is more or less isolated for the two wings. The same transition from squeeze–peel to ‘near clap and fling’ (Ellington 1984*a*) was observed by Götz (1987*a*) for *Drosophila* flying in a head wind. The kinematic modifications of the squeeze–peel are summarized in figure 7*d*. At wind speeds of  $0.5 \text{ m s}^{-1}$  (middle row), an intermediate behaviour is observed.

The ‘football’ projection (right column of figure 2) demonstrates how the overall shape of the wing path is influenced by the wind. In still air, the wing trajectory resembles a curved ‘figure-of-eight’ with the upstroke situated in front of the downstroke in the large ventral loop and behind the downstroke in the small dorsal loop. Exposed to an air speed of  $1 \text{ m s}^{-1}$ , the upstroke is close behind the downstroke in the large dorsal loop of the ‘figure-of-eight’ and in front of the upstroke only driving a short time near the ventral reversal point. Thus, with the

CONTROL OF *DROSOPHILA* WING BEAT

51

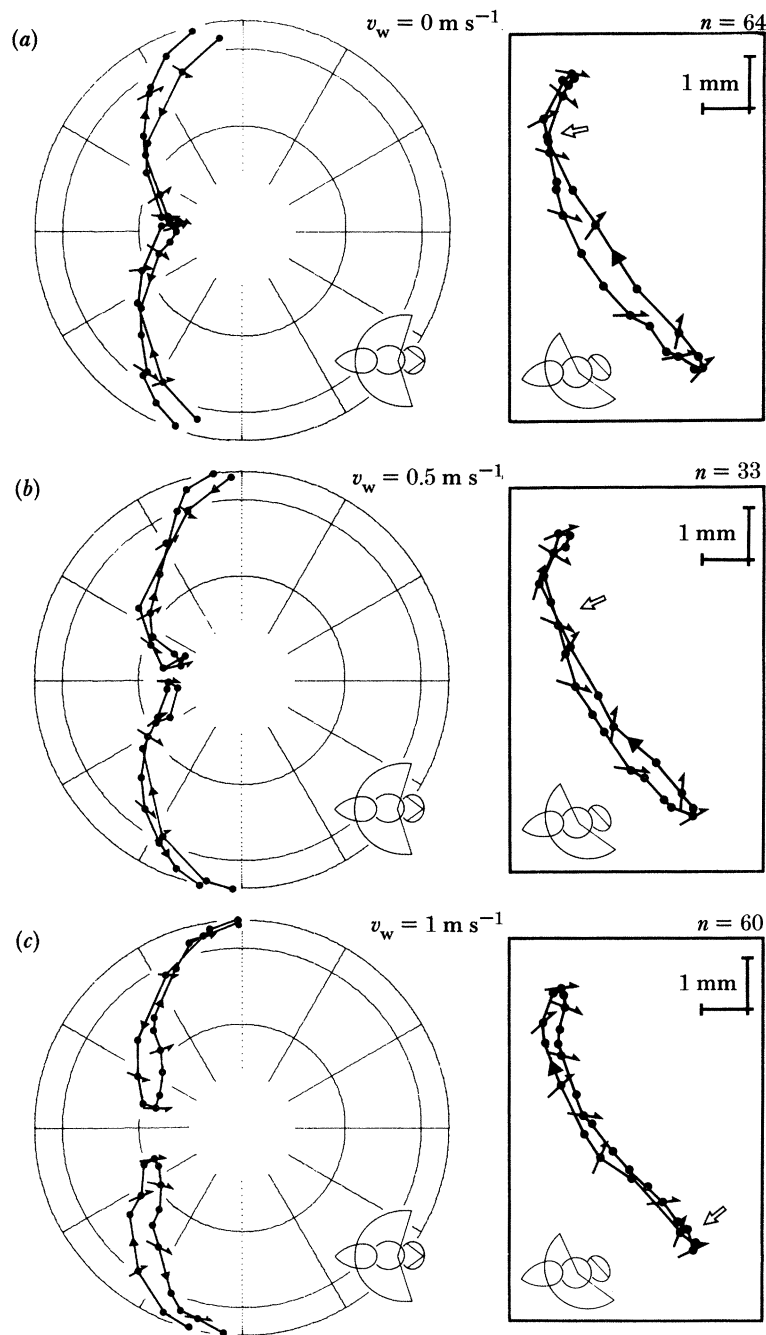


FIGURE 2. Wing path during wind stimulation in dorsal parallel projection (left column) and lateral ‘football’ projection (right column) described in paper 1. (a) In still air ( $v_w = 0 \text{ m s}^{-1}$ ), the wings touch each other during the dorsal reversal and perform the ‘squeeze-peel’. The upstroke path intersects with the downstroke path in the dorsal region (open arrow in ‘football’ projection). (b) At moderate wind speeds ( $v_w = 0.5 \text{ m s}^{-1}$ ) the wings still touch each other dorsally. The wing-path loop becomes narrow because the upstroke is shifted caudally and, correspondingly, the intersection point between upstroke and downstroke is lowered. (c) In strong head wind ( $v_w = 1.0 \text{ m s}^{-1}$ ) the wings do not touch each other during the dorsal reversal and the supination of either wing is isolated from the other. The intersection point is shifted to the ventral end of the wing-path loop.



intersection point situated close to the ventral end of the path (open arrow in figure 2*c*), the ventral loop almost disappears. Again, at wind speeds of  $0.5 \text{ m s}^{-1}$ , the behaviour is intermediate. In this case, the upstroke path intersects with the steeper downstroke path somewhere in the dorsal half (open arrow in figure 2*b*). To summarize, the intersection point of the upstroke path with the steeper downstroke path is displaced with increasing wind speed from the dorsal to the ventral region (open arrows in figure 2). A simple explanation for such displacements can be derived from the frictional forces acting on the wings. During the upstroke the *morphological* angles of attack (the angle between the transverse axis of the wing and the horizontal) are much bigger than during the downstroke; thus the head-wind pressure acts on an increased profile surface area, and the wings will be shifted more caudally, during the upstroke. This observation adds a new aspect to the old discussion of the wing path's shape. Nachtigall (1966), for instance, reported a figure-of-eight path in still air for the blowfly *Phormia*, whereas the wings moved on an ellipsoid in the wind. In contrast, the flies *Musca* and *Muscina* move their wings on a figure-of-eight path in the wind, but on an ellipsoid in still air (Hollick 1940). In all flies, however, the head wind is shifting the upstroke path caudally with respect to the downstroke. Thus the relative position of upstroke and downstroke might be a more consistent indicator of changes of the wing path than the transition between ellipsoidal or figure-of-eight-shaped trajectories of the wings. Actually, the simple explanation is challenged by the observation that in *Muscina* the paths appeared to be similar in still air and in wind, if the antennae of the fly were immobilized (Hollick 1940). Changes mediated by the sensory input from the antennae cannot be attributed to passive changes in the air friction of the wings.

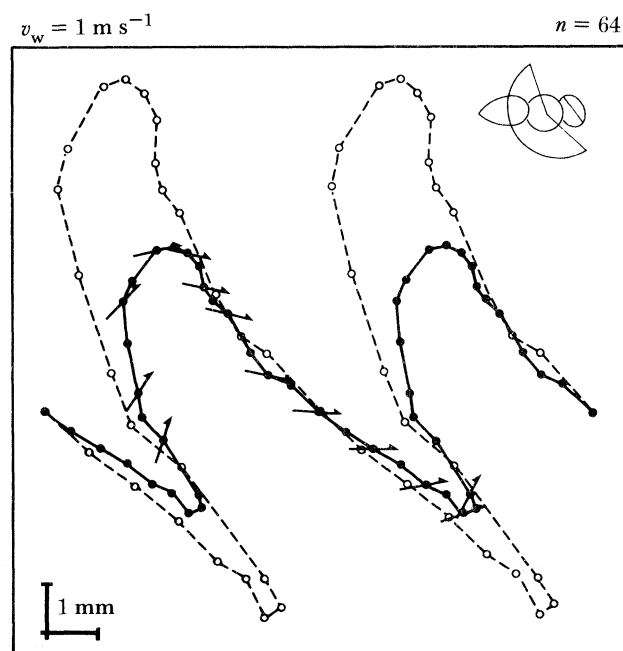


FIGURE 3. Wing path with respect to the air in head wind on the 'football' projection, including the additional wind velocity component of  $1 \text{ m s}^{-1}$ . (Data as in figure 2*c*.) Despite the considerable translational speed of the complete animal relative to the air, the wing still moves backwards during upstroke both at its centre (black dots) and its tip (open circles). Accordingly the distal part of the wing is touched by the air from its anatomical upper surface during that phase of the wing-beat cycle.

An illustration of the relative motion between the wing and the air has to account for the wind stimulus. This is done by adding the wind speed ( $1 \text{ m s}^{-1}$ ) to the horizontal coordinates in the ‘football’ projection of figure 2*c*, now showing the average motion of the wing’s centre of gravity (black dots and continuous line in figure 3) or of the wing tip (open circles and broken lines) relative to the air. It can be seen immediately, that the outer part of the wing is moving backwards during the upstroke and is therefore still touched by the wind from its anatomical top side. Comparison of figures 2*a* and 3 (both describing wing motion with respect to the coordinates of a zero-wind-speed system) demonstrates that during the downstroke (upstroke) the *aerodynamic* angle of attack (the angle between the path of the wing element and its transverse axis, indicated by the arrows) decreases (increases) on transition from hovering to fast forward flight. Note that without any further active or passive alterations of the wing-bat kinematics, the additional velocity component of head wind is sufficient to change both the aerodynamic angles of attack and the aerodynamic effective velocities.

These observations led us to a quantitative analysis of kinematic and aerodynamic parameters (figure 4). The major change of wing-beat path, i.e. the reduced elevation during the dorsal reversal phase, is reflected by the smaller average wing-beat amplitude of  $132^\circ$  in wind, compared to  $145^\circ$  in still air. (Wing-beat amplitudes are calculated in the average stroke plane, inclined by  $120^\circ$  relative to the body horizontal.) The *morphological* angles of attack,  $\alpha_m$ , plotted in figure 4*a* as function of non-dimensional time, and correspondingly the rotational speed of the wing (not displayed), seem to be virtually unchanged by the wind. This is interesting because the wind would be expected to increase the pressure on the wings, particularly when the wings have high angles of attack. A flag-like wing would adapt to this situation by reducing its inclination. The constancy of the pronation and supination angles suggest that the angle of attack is actively stabilized or that the axis of rotation and pronation lies near the centre of the wing spread.

In contrast to the virtually unchanged morphological angle of attack,  $\alpha_m$ , the amount of *aerodynamic* angle of attack,  $\alpha_a$ , is generally reduced in the wind (black dots and triangle in figure 4*b*). As mentioned above, this reduction is due to a change of the path of the wing elements with respect to the air. This is shown by the following control calculation which will be used later to isolate the effects of purely kinematic changes (active or passive) from those due to wind. By computing the aerodynamic variables from the kinematic data obtained in still air, under the assumption of a fictive wind  $v_{\text{fict}}$  of the same size as in the experiments with head wind, the effect of wind-induced components in the absence of kinematic responses can be estimated. These values have to be compared with the results of the corresponding calculations for the wind experiments, in order to assess the relevance of the kinematic responses to the wind. In figure 4*b* the result for the aerodynamic angle of attack is presented. The timecourse of  $\alpha_a$  for a fictitious wind ( $v_{\text{fict}} = 1 \text{ m s}^{-1}$ , open circles) resembles more the time course for actual wind stimulation ( $v_w = 1 \text{ m s}^{-1}$ , triangles), than that for still air ( $v_w = 0 \text{ m s}^{-1}$ , dots). Significant differences between  $\alpha_a$  for fictitious and actual wind can only be identified during the dorsal reversal phase (shaded area in figure 4*b*). Thus, most modifications of the aerodynamic angle of attack are due to the additional wind velocity component, not to kinematics. The same basic result was found for the aerodynamic effective velocity  $v_a$ , which is increased in wind during almost the complete wing-beat cycle, compared with still air (figure 4*c*). Again, however, a very similar timecourse was derived from the still air data, if a fictitious wind is assumed. As shown by the shaded areas in figure 4*c*, this increase is even stronger than in actual wind. The

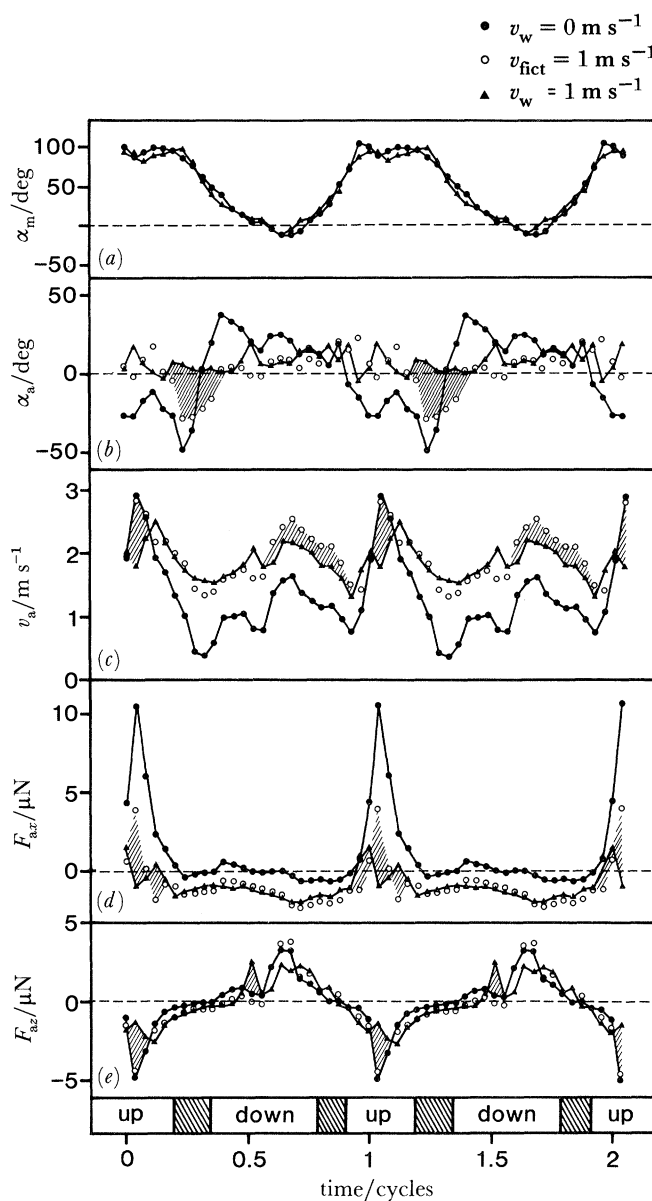


FIGURE 4. Aerodynamic variables as functions of non-dimensional time (fractions of the wing-beat cycle; the four phases of a cycle are indicated by the 'event scale' on the bottom) obtained either in still air ( $v_w = 0 \text{ m s}^{-1}$ , black dots, 46–68 values averaged per phase-step bin), or during head wind ( $v_w = 1 \text{ m s}^{-1}$ , black triangles, 52–74 values averaged per phase-step bin), or calculated for the data for still air under the assumption of a fictitious air flow of the same size ( $v_{\text{fict}} = 1 \text{ m s}^{-1}$ , open circles). The s.e.m.s are given as the average values for all 25 phase-step bins and all three stimulus conditions. (a) The *morphological* angle of attack  $\alpha_m$  is very similar in still air and during head wind stimulation (average s.e.m.  $\pm 5.3^\circ$ ). (b) The amount of the *aerodynamic* angle of attack  $\alpha_a$  (average s.e.m.  $\pm 5.0^\circ$ ) is generally reduced in the wind. This is a consequence of the path of the wing elements with respect to the air, since a similar effect can be observed for fictitious wind, except for the reversal phase between the upstroke and downstroke (shaded areas). (c) The aerodynamic velocity  $v_a$  (average s.e.m.  $\pm 0.09 \text{ m s}^{-1}$ ) is generally increased by the additional wind-velocity component. During the lower downstroke and median upstroke of the wing-beat cycle, however,  $v_a$  appears to be reduced in the actual wind, as compared to  $v_a$  calculated for fictitious wind (shaded areas). (d) The horizontal aerodynamic force component per wing, calculated according to the quasi-steady theory,  $F_{ax}$  (average s.e.m.  $\pm 0.33 \mu\text{N}$ ), is generally shifted to smaller, more negative values for actual or fictitious wind. Irregular differences between the forces at real and fictitious wind can be observed during the upstroke (shaded areas). (e) The vertical component of the quasi-steady aerodynamic force,  $F_{ay}$  (average s.e.m.  $\pm 0.43 \mu\text{N}$ ), are affected only slightly by the wind; short intervals of flight force increase can be observed during head-wind stimulation (shaded areas).

increase of  $v_a$  is mainly caused by the additional wind velocity component, not by changes of wing-beat kinematics.

TABLE 1. FLIGHT FORCES AVERAGED OVER THE WING-BEAT CYCLE, CALCULATED ACCORDING TO THE QUASI-STATIONARY THEORY FOR ONE WING

(Head wind stimulus: ' $v_w = 0, 0.5$ ', denote head wind speeds of 0, 0.5, 1 m s<sup>-1</sup>; ' $v_{\text{fict}} = 1$ ' denotes the control calculation assuming fictitious head wind. Visual stimulus: the notation relates to the direction of pattern movement seen on the ipsilateral side of the wing: 'yaw progr.' and 'yaw regr.' denote front-to-back and back-to-front drifting patterns; 'roll up' and 'roll down' refer to the side where the stripes move upwards and downwards during the rotation of the patterns; 'pitch up' and 'pitch down' denote upwards and downwards pattern motion. The mean number of measurements per phase step is given by ' $\bar{n}$ ' and the wing-beat amplitude in the average stroke plane by 'stroke ampl.' The average flight forces are presented by their horizontal ( $\overline{F_{ax}}$ ) and vertical ( $\overline{F_{az}}$ ) components, which are converted into their average magnitude ( $|\overline{F_a}|$ ) and inclination relative to the body ( $\alpha_{F_a}$ ).

	stroke ampl.	$\overline{F_{ax}}$	$\overline{F_{az}}$	$ \overline{F_a} $	$\alpha_{F_a}$	
stimulus	$\bar{n}$	deg	$\mu\text{N}$	$\mu\text{N}$	$\mu\text{N}$	deg
$v_w = 0$	60	145	0.90	0.16	0.91	10
$v_w = 0.5$	33	142	0.10	0.09	0.14	42
$v_w = 1$	64	132	-0.88	0.06	0.88	176
$v_{\text{fict}} = 1$	60	145	-0.92	-0.01	0.92	-181
yaw progr.	39	140	0.81	0.28	0.86	19
yaw regr.	39	147	0.81	0.31	0.87	21
roll up	38	143	0.75	0.29	0.80	21
roll down	38	146	0.71	0.31	0.78	24
pitch up	39	143	0.78	0.36	0.86	25
pitch down	38	143	0.78	0.26	0.82	18

Because the increase of the aerodynamic velocity and the decrease of the aerodynamic angle of attack act antagonistically on the magnitude of the aerodynamic force, it is not obvious how the expected output force of the flight motor will vary with external wind speed. The horizontal and vertical components of the aerodynamic force,  $F_{ax}$  and  $F_{az}$ , calculated according to the quasi-steady assumption for a single wing, are plotted in figure 4 (*d*, *e*) as functions of non-dimensional time. The horizontal force component is strongly reduced during the upstroke, leading to a time average for a wing pair of  $-1.76 \mu\text{N}$  in wind, compared with  $1.80 \mu\text{N}$  in still air (see table 1). At first glance this looks like a compensatory response, which reduces the thrust with increasing airspeed. However, the separation of the effects of the additional velocity component and the kinematic alterations due to the wind do not support this conjecture. The control calculation for fictitious wind in the absence of kinematic alteration predict an even stronger thrust reduction (see open circles in figure 4*d*, and table 1 for time average). Accordingly, the fly responds to wind with an increase, not decrease, of the forward-directed flight-force component. In free flight, the response would increase rather than decrease the actual air speed. The vertical force component seems not to be affected significantly by the wind. Small increases of  $F_{az}$  occur during short time intervals of both upstroke and downstroke (shaded areas in figure 4*e*) which are not expected for fictitious wind. However, these effects may be due to statistical fluctuations of single data points (cf. the corresponding deviations of single points in the plots of  $v_a$ ). After all, there seems to be a small effect of air speed on the average vertical force (see table 1) which is in between  $\overline{F_{az}}$  expected in still air and  $\overline{F_{az}}$  expected in fictive wind. This again suggests reinforcement of the flight motor output in wind, according to the quasi-steady aerodynamic theory.

If we accept the view that quasi-steady theory is not sufficient to explain the flight-force generation of small flapping wings, we are no longer surprised that speed control cannot be explained by this theory satisfyingly, either. If we content ourselves with a more qualitative, but perhaps more realistic, view of control mechanisms instead, solutions to our problems are obvious. The transition from the clap–fling to isolated pronation of the two wings would suggest a reduction of flight force production by wing interference during the dorsal reversal (see figure 7*d*). In addition, less pronounced variations of the geometry and/or speed of the ventral ‘quick rotation’ which was proposed to play a major role in force generation (see paper 2) could possibly be used by the fly to vary the flight forces, to counteract increased air speeds. The observation that in wind the rotational speed during the quick rotation is about 10% smaller than in still air, points in this direction.

(*b*) *Response to visual stimuli*

To ease the evaluation of the visual responses, the data sets were averaged according to the following assumptions about the symmetry of the control system. Yaw and roll stimuli are antisymmetrical with respect to the sagittal plane of the fly and therefore were expected to elicit opposite responses at the two wings, whereas the symmetrical pitch stimuli were expected to elicit the same basic responses at both wings. These expectations were verified by qualitative comparison of the data samples before averaging. Three pairs of data sets are derived for the three pairs of stimulus conditions (see bottom of figure 5): (i) ‘yaw progressive’ (‘yaw regressive’) denotes the data from that side of the fly where the gratings move front-to-back (back-to-front) which is the left (right) wing for right-to-left or the right (left) wing for left-to-right pattern motion. (ii) ‘Roll up’ (‘roll down’) denotes the data from that side of the fly where the roll stimulus moves upwards (downwards), which is the left (right) wing for clockwise or the right (left) wing for anticlockwise pattern rotation. (iii) ‘Pitch down’ (‘pitch up’) denotes the pooled data from both wings for gratings moving downwards (upwards). One should keep in mind that by separate treatment of the left and right wing (stimulus conditions (i) and (ii)) the symmetry assumptions used in the kinematic analysis could be violated. To correct for misalignments of the fly, we rotated the wing-axis data sets such that they were approximately symmetrical for the two wings (see paper 1). If in asymmetrical stimulus conditions, such as yaw or roll, both wings shift their average position to one side, for instance, this kinematic change would be annihilated in the present analysis by the symmetry-restoring procedure. However, all average differences between the symmetry-restoring rotations for the opposing stimuli (such as clockwise versus anticlockwise stripe rotations) are smaller than 2.5°. The only value significantly different from zero ( $p < 0.05$ , Student’s *t*-test) is a rotation of 1.6° to the right for stripe movement to the right, compared with the rotation for stripe movement to the left. Thus, the systematic errors introduced by the corrections used in the kinematic analysis are very small and may be neglected in a first approximation.

A first impression of the kinematic adaptations to the various stimulus conditions can be derived from the wing paths plotted in figure 5 as football projection (see paper 1). It is obvious from figure 5*a* that *yaw* stimuli lead to an extension of the wing path ellipsoid on that side of the fly where the pattern is moving back to front. As expected (Götz 1968; Götz & Wandel 1984), neither the angles of attack nor the inclination of the average stroke plane are influenced considerably by the stimulation. The extension of the wing path corresponds to a wing-beat amplitude (again calculated in the average stroke plane inclined 120° relative to the body

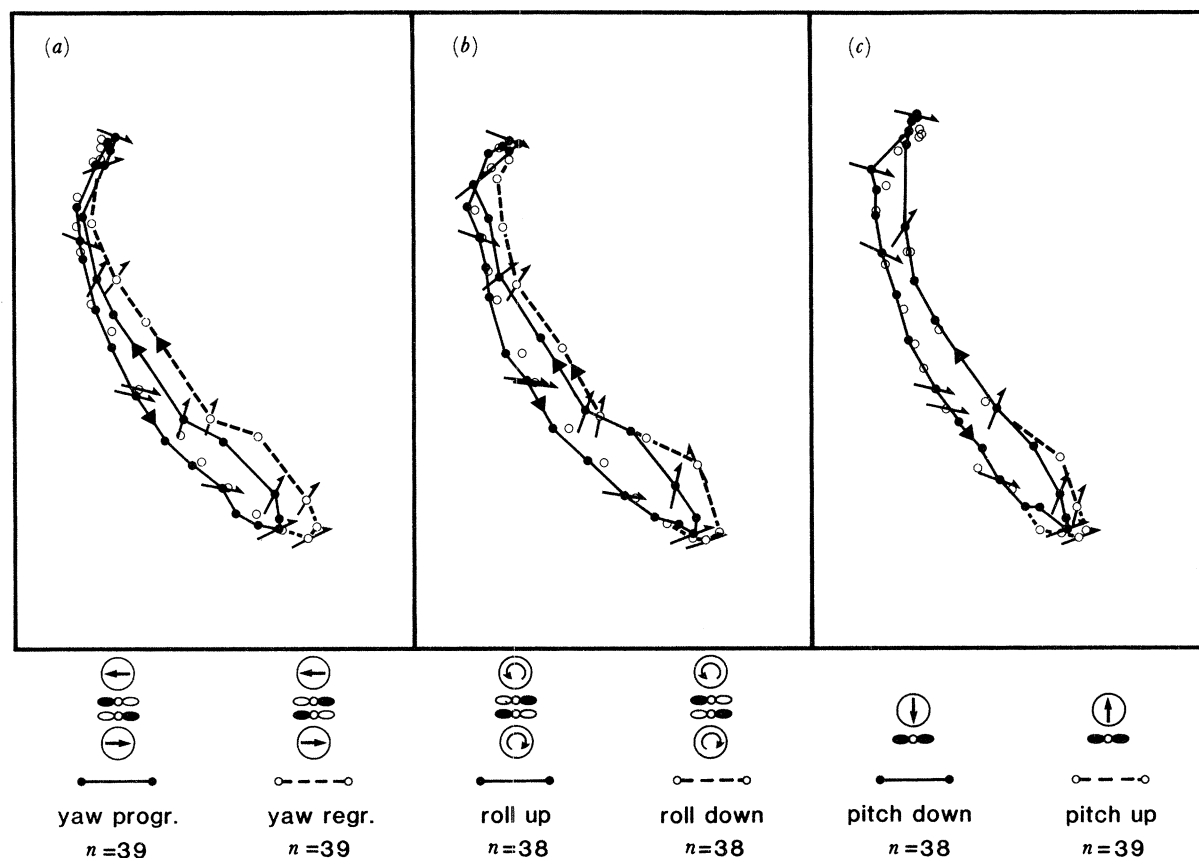


FIGURE 5. Wing paths during visual stimulation. The fly symbols on the bottom illustrate which of the two wings (black) is included in the averages for a given stimulus (arrows). (a) During horizontal pattern motion the ellipsoid of the wing path is extended and the upstroke is shifted frontally on the side of back-to-front pattern motion ('yaw regr.', open circles), compared with the side of front-to-back pattern motion ('yaw progr.', black dots). (b) When the pattern rotates on the screen in front of the fly, the wing-path loop is slightly extended ventrally and the upstroke is slightly shifted frontally on the side of downwards pattern motion ('roll down', open circles), compared with the side of upwards pattern motion ('roll up', black dots). (c) When the gratings move upwards ('pitch up', open circles) the stroke of either wing is slightly reduced near the dorsal region and slightly extended in the ventral region, compared with downwards pattern motion ('pitch down', black dots).

horizontal) of  $147^\circ$  on the side of regressive pattern motion, compared with  $140^\circ$  on the side of progressive pattern motion. This difference of wing-beat amplitudes is not as big as the values described in the literature (*ca.*  $10^\circ$  (Götz 1983)). The visual system might be disturbed in the present experiments by the light flashes used for filming the flies, which could reduce response amplitudes considerably. Nevertheless, the wing-beat amplitude responses were consistent and significant, suggesting that the stimuli were sufficient to elicit control responses. This view was confirmed by simultaneous observation of abdominal deflections to the side of progressive pattern motion, an independent course-control mechanism expected in response to the visual yaw stimulus (Götz *et al.* 1979; Zanker 1988*b*).

As can be seen in figure 5*b*, *roll* stimuli extend the wing path on the side of downwards pattern motion. The corresponding amplitude difference of  $3^\circ$  is even smaller than that elicited by yaw stimuli. No obvious changes in the angles of attack could be observed. Finally, in figure 5*c* the slight ventral extension of the wing path for *pitch* up stimuli is illustrated. The

corresponding difference between the wing beat amplitudes of the two wings is below  $1^\circ$  (see table 1), apparently because the ventral extension is compensated by a dorsal reduction of wing-beat amplitude during upwards pattern motion. Again the angles of attack seem to be virtually unchanged.

In the following, the changes of the kinematic and aerodynamic variables are discussed in some detail for the yaw stimulation, whereas for the other stimuli, apparently even less effective, only the net effects on the size and orientation of the resulting average flight force vectors (listed in table 1) will be considered.

The time course of the relevant kinematic and aerodynamic variables are displayed in figure 6 for the two yaw stimulus conditions of progressive (black dots) and regressive (open circles) pattern motion. During a major part of the wing-beat cycle the morphological angle of attack  $\alpha_m$  is slightly increased for regressive pattern motion, interrupted by short intervals of reduced  $\alpha_m$ ; however, these differences are extremely small. Larger changes can be identified in the aerodynamic angle of attack,  $\alpha_a$ . With the exception of the ventral reversal phase this angle is slightly increased for progressive pattern motion, i.e. almost the complete curve is shifted to more positive values (shaded areas in figure 6*b*). The aerodynamically effective velocity  $v_a$  does not seem to differ strongly between the two wings, except for the end of downstroke, where it is slightly increased on the side of regressive pattern motion (shaded areas in figure 6*d*). This increase of  $v_a$  is due to the extended wing path and appears to be the major effect of the increased wing-beat amplitude. Despite these changes in the variables determining the aerodynamic forces, the time courses of the calculated horizontal and vertical flight-force components (figure 6*e, f*) are almost indistinguishable for the two wings. Also, the time averages (see table 1) are very close to each other; the mean flight force in the sagittal plane is increased about  $0.01 \mu\text{N}$  on the side of regressive pattern motion.

The increase of flight force on the side of back-to-front pattern motion could be interpreted as compensatory response, as it would reduce the retinal speed of this stimulus in free flight. However, the magnitude of the calculated response is negligible. Assuming a lever arm of maximum  $0.002 \text{ m}$  (i.e.  $0.0005 \text{ m}$  thorax radius and  $0.0015 \text{ m}$  distance of the average flight force vector from the wing base) a torque of about  $0.04 \times 10^{-9} \text{ N m}$  is derived. This is small compared with the average torque of  $2.10^{-9} \text{ N m}$  per wing measured under corresponding stimulus conditions, even if one takes into account that in these experiments the wing-beat amplitude response is about twice as strong (Götz 1968, 1983). In addition, the difference between the flight forces on either side is confined to the vertical components (see table 1), i.e. the yaw stimulus would lead to lift differences on the two sides which would induce a roll instead of a yaw torque. Torque estimates based on time-averaged forces, and an average lever arm are likely to deviate from the actual values. A better estimate should take into account the instantaneous values of all three force components and the exact wing positions associated with them. Indeed, when the average torques about all three body axes are calculated from the instantaneous data obtained during yaw stimulation for either wing, the result is somewhat different. The *yaw* torque generated on the side of regressive pattern motion ( $1.04 \times 10^{-9} \text{ N m}$ ) and on the side of progressive motion ( $-1.10 \times 10^{-9} \text{ N m}$ ) cancel each other almost completely. A very small torque remains which would rotate the fly in the opposite direction to the pattern motion, thus increasing the retinal slip. The *roll* torque difference between the wings on the side of regressive and progressive pattern motion ( $0.63\text{--}0.54 \times 10^{-9} \text{ N m}$ ) would rotate a fly to the inner side of a compensatory curve, such as observed during ‘banked turns’.

CONTROL OF *DROSOPHILA* WING BEAT

59

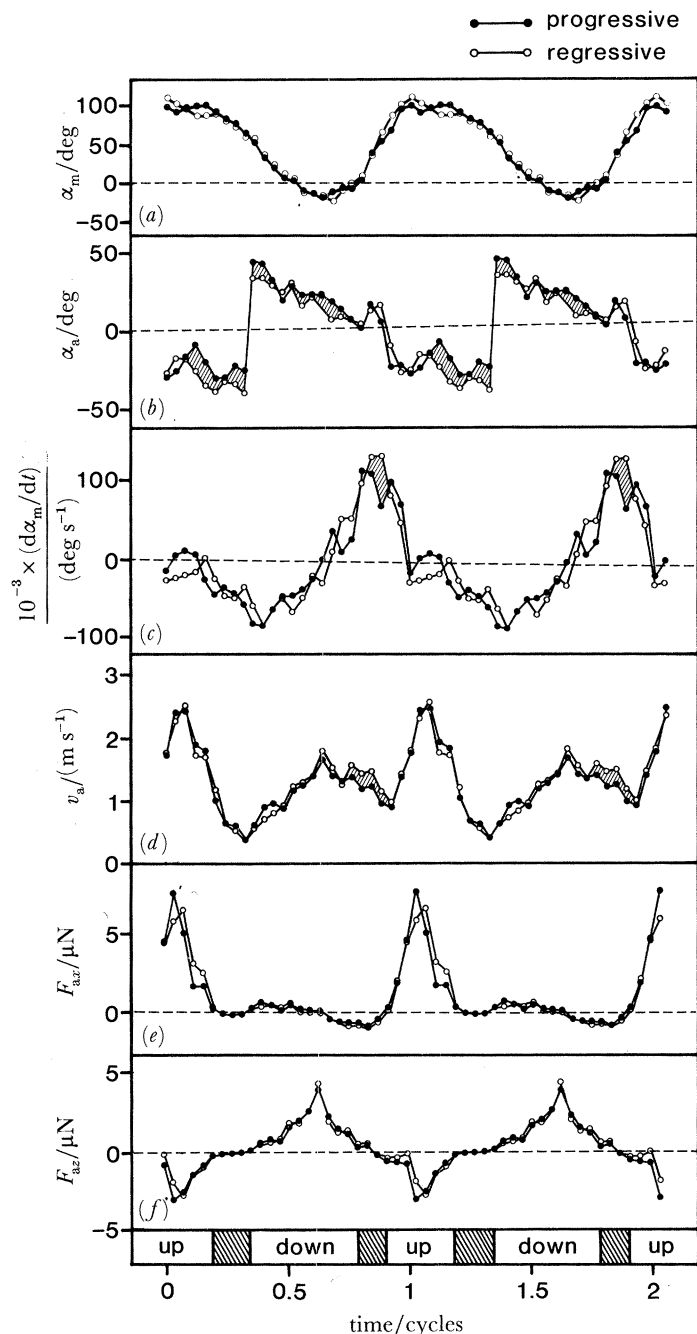


FIGURE 6. Aerodynamic variables as function of non-dimensional time (fractions of the wing beat period, the four phases of a cycle are indicated by the 'event scale' on the bottom) for front-to-back pattern motion ('progressive', black dots) and for back-to-front pattern motion ('regressive', open circles). Standard errors of the mean are given as mean values for all 25 phase-step bins and both stimulus conditions, with 30–45 single values averaged in each phase-step bin for each stimulus condition. (a) The *morphological* angle of attack  $\alpha_m$  (average s.e.m.  $\pm 5.2^\circ$ ) is slightly increased at the beginning and slightly decreased at the end of the upstroke for regressive pattern motion. (b) The *aerodynamic* angle of attack  $\alpha_a$  (average s.e.m.  $\pm 6.9^\circ$ ) is generally reduced for regressive pattern motion (shaded areas). (c) The rotational speed of the wings  $d\alpha_m/dt$  (average s.e.m.  $\pm 16.10^3 \text{ deg s}^{-1}$ ) is very similar for both wings, except for a slight reduction of the peak velocity during the ventral reversal for progressive pattern motion (shaded areas). (d) The aerodynamic velocity  $v_a$  (average s.e.m.  $\pm 0.12 \text{ m s}^{-1}$ ) is generally very similar for both wings, except for a slight increase during the final downstroke for 'regressive' pattern motion (shaded areas). (e, f) Despite all the differences, the horizontal and vertical aerodynamic force components per wing, calculated according to the quasi-steady theory,  $F_{ax}$  and  $F_{ay}$  (average s.e.m.  $\pm 0.44 \text{ }\mu\text{N}$  and  $\pm 0.43 \text{ }\mu\text{N}$ ), are very similar for both wings.



These two contradictory results are further obscured by the average pitch torques generated by each of the two wings during the same stimulus conditions ( $0.43 \times 10^{-9}$  N m). They would continuously rotate the fly nose down, if the centre of gravity is near to the wing bases. In summary, these calculations indicate that a flying machine like *Drosophila* would be unstable if it worked according to the quasi-steady aerodynamic theory.

Finally, for the yaw stimulus being asymmetrical with respect to the sagittal plane of the fly, the mean *transverse* force components,  $F_{ay}$ , have to be considered, which do not annihilate each other as during symmetrical stimulation. In all cases, the mean  $F_{ay}$  on either side is directed towards the body of the fly. The force component for regressive pattern motion ( $0.16 \mu\text{N}$ ) exceeds the force component for progressive pattern motion ( $0.12 \mu\text{N}$ ). This could be interpreted as a compensatory response reducing the simulated translation along the transverse body axis by generating a sideslip component. However, the magnitude of the effect is too small to be considered as a significant response. The differences between the transversal force components obtained under *symmetrical* stimulus conditions were found to be in the same order of magnitude.

In conclusion, an explanation of the functional role of stimulus-induced kinematic changes in wing beat according to the quasi-steady aerodynamic theory seems to be impossible. Accordingly, the unsteady effects of the kinematic changes must be considered. Two observations have to be mentioned in this context. (i) The mean orientation of the wings during the dorsal clap–fling process is not parallel to the sagittal plane of the fly. An effect of the squeeze–peel, complementary to circulation changes, is a jet of air which is ejected backwards and conclusively propels the fly forwards (Ellington 1984*d*). If this jet of air, and the corresponding flight force, does not act parallel to the longitudinal body axis on the centre of gravity but obliquely and somewhere behind the centre of the fly, it should generate a torque about the vertical body axis. A deflection of the wing chord's bisector parallel to the abdomen deflections was reported by Götz (1987*a*) and interpreted correspondingly. The white arrows in figure 7*a* show that during yaw stimulation the bisector between the wings is indeed directed slightly to the side of regressive pattern motion. (The magnitude of this effect is likely to be underestimated in the present experiment, because of the small rotation introduced by symmetry-restoring procedure described above). Because the wings are far behind the position of the wing base (indicated by the cross in figure 7), it seems realistic to assume an intersection point for the instantaneous force vector with the longitudinal body axis behind the centre of gravity. In this case, the fly would be rotated in free flight syndirectional with pattern motion, thus reducing the retinal slip. So far, no quantitative conclusions can be drawn because neither the magnitude of the unsteady flight force nor the lever arm can be estimated satisfyingly. (ii) As shown in figure 6*c*, the time course of the quick rotation during the ventral reversal is different for the two wings: the supination is faster on the side of regressive pattern motion (the data suggests a 15% increase of the peak rotational speed). According to the proposition that flight force is generated by vortex shedding during that phase of the wing-beat cycle, differences in the dynamics of wing rotation, and in the corresponding vortex shedding, could result in a torque component that reduces the simulated course deviation from a straight course. Again, no quantitative estimates are available at this stage.

In contrast to observations on *Calliphora* during visual and mechanical *roll* stimulation (Hengstenberg *et al.* 1986), the angles of attack are not influenced significantly during frontal visual stimulation of *Drosophila*. The difference between the angles  $\alpha_m$  ( $\alpha_a$ ) of the wing on the

side of the 'roll down' stimulus,  $-8.2^\circ$  ( $16.4^\circ$ ), and the wing on the side of the 'roll up' stimulus,  $-7.8^\circ$  ( $16.9^\circ$ ), are negligible. This discrepancy can either be due to interspecific differences, or to the restriction of the stimulus to the frontal visual field of the flies in the present experiment. The average response to roll stimuli (see table 1) is a slight decrease in the wing-beat amplitude on the side of upward pattern motion ( $143^\circ$ ), compared with the side of downward pattern motion ( $146^\circ$ ). This contradicts the calculated average flight force, which increases on the side of upward movement and decreases on the side of downward movement. The calculated forces correspond to a compensatory response, which was actually measured in *Drosophila* (Blondeau & Heisenberg 1982) but which is much stronger than the torques expected from the calculated force differences. Interestingly, the simple correlation between the amplitude of the wing beat and the average flight force found in experiments on yaw- and lift-control (Götz 1968, 1983; Götz *et al.* 1979) is not obtained under the conditions of the quasi-steady theory. When comparing the *horizontal* and *vertical* components of average flight forces calculated for the two sides according to the quasi-steady theory, it turns out that the major difference exists between the horizontal components (i.e. the roll stimulus preferentially elicits a yaw response) and that the vertical component is decreased on the side of upwards pattern motion (i.e. the roll response is not compensatory). Again, these paradoxical results are not surprising, if one accepts that the major effects of wing beat are not adequately described by the quasi-steady theory. A qualitative analysis of the squeeze-peel events in roll stimulation does not lead to meaningful suggestions such as those for yaw stimulation. The bisector of the wings' transversal axes, and correspondingly, the expected unsteady flight force, does not show any consistent orientation.

The changes of wing beat amplitude elicited by *pitch* stimuli are extremely small ( $0.7^\circ$ ; see table 1). However, in this case the average flight forces calculated according to the quasi-steady theory suggest a compensatory response. Frontal stimulation by pattern movement in upward or downward direction can be attributed to pitch movements as well as to vertical displacements of the fly. In this context, losing (gaining) height, as indicated by upwards (downwards) pattern motion of the visual surroundings, leads to an average vertical force component of  $0.36$  ( $0.26$ )  $\mu\text{N}$ . However it is questionable whether the size of this altitude control response could account for height stabilization in free flight. Indeed, the lift difference actually measured under similar stimulus conditions (Götz 1983) is an order of magnitude bigger than the difference calculated here. Interestingly, the extent of contact between the two wings (figure 7c), i.e. the strength of the squeeze-peel, seems to be increased for gratings moving downwards compared with gratings moving upwards (the extended contact corresponds to the slight dorsal increase in the wing-beat amplitude in figure 5c). This increases the flight force produced dorsally in response to pitch-down stimuli. Such a response is expected not to counteract but to reinforce the simulated ascending of the fly, as long as it will produce a force component directed upwards. On the other hand, it is likely to be used in pitch control. Because the flight force is increased dorsally, a freely flying fly would pitch nose down, thus decreasing the vertical displacement of the retinal image, if other mechanisms were not affected.

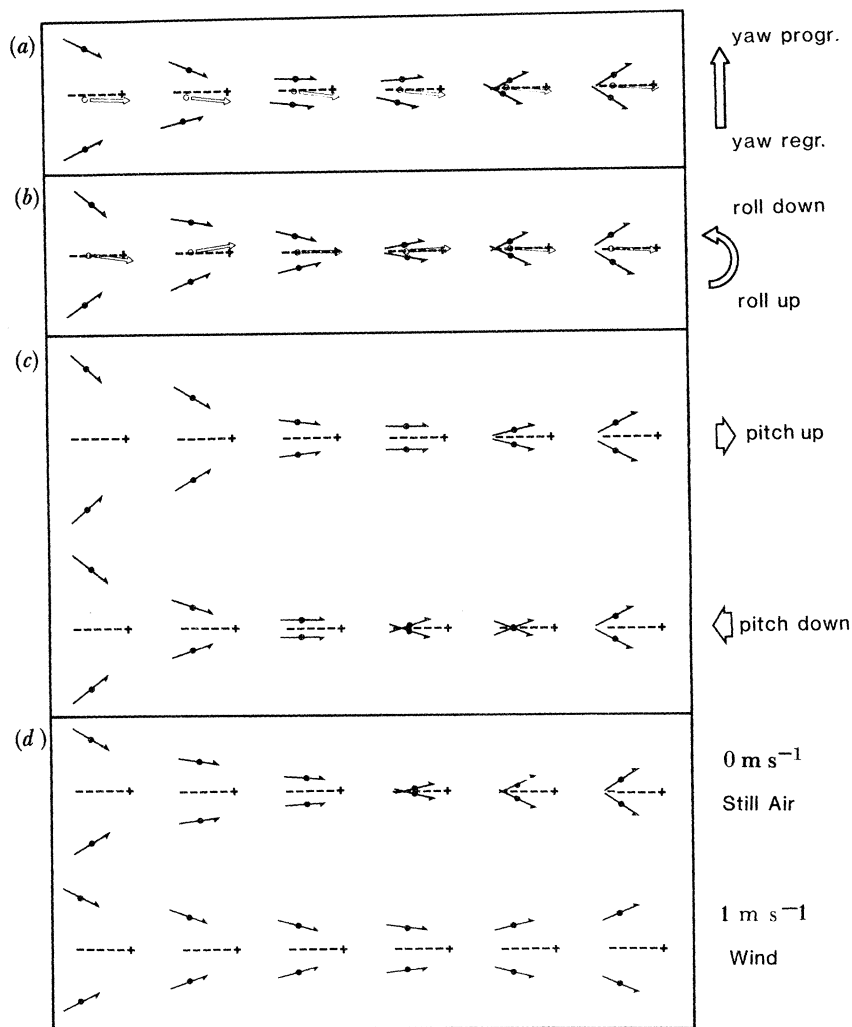


FIGURE 7. Adaptations of squeeze-peel at the dorsal reversal of the wing beat to various stimulus conditions, shown in six subsequent steps, each representing  $\frac{1}{35}$  of the wing-beat cycle. The transversal wing axes of the wings, as seen in top view, are symbolized by the thin arrows. The orientation of the fly and its centre (represented by the midpoint of the wing base interconnection) is given by a broken line and a cross, respectively. The open circle denotes the midpoint between the centres of gravity of the two wings. (a) During yaw stimulation the bisector of the two wings (open arrow) is not parallel to the longitudinal body axis but directed to the side of back-to-front pattern motion. The flight force produced by the squeeze of air to the rear is expected to generate torque about the vertical axis through the centre of the fly. (b) No significant asymmetry between the transverse axes of the two wings has been found during roll stimulation. (c) Downwards pattern motion increases (upward motion decreases) the extent of the contact between the two wings. This could correspond to an increased (decreased) force generation, at the dorsal reversal, which would pitch the fly nose down (nose up). (d) In the wind, the wings no longer touch each other, possibly leading to a reduction in the average flight force production. Note that in (c) and (d) the perfect mirror symmetry between the two wings is due to the use of the same set of data for the left and right wing. The effects shown in (a) and (d) confirm earlier observations (Götz 1987a).

#### 4. CONCLUSIONS

This third part of the present series of papers deals with the wing-beat responses expected from quasi-steady aerodynamic evaluation of the recorded kinematic changes elicited by various stimuli simulating flight perturbations. Although there seems to be little doubt left that quasi-steady theory cannot explain basic aspects of flight force production (for discussion, see

paper 2), we wanted to test whether control responses of the *Drosophila* wing-beat cycle could be understood on such a simplifying theoretical background. In general, the adaptations of flight forces expected from quasi-steady aerodynamics are either very small compared with actual force and torque measurements (Götz 1968, 1983; Blondeau & Heisenberg 1982), or even paradoxical in that they would not compensate but even exaggerate the visual or mechanosensory stimuli. These results are not surprising if one remembers that the force of flight produced in *Drosophila* seems to be dominated by unsteady effects not covered by the quasi-steady aerodynamic theory (Ellington 1984*d*; Zanker & Götz 1990). However, from the present investigation it is now clear that quasi-steady theory as developed so far fails to account for flight-force production as well as for flight control.

Alternatively, control reactions have to be considered on the basis of the major unsteady processes, such as the dorsal squeeze–peel (Weis-Fogh 1973; Ellington 1984*d*; Götz 1987*a*) and the ventral quick rotation (Zanker & Götz 1990). The changes in *squeeze–peel* kinematics are summarized in figure 7. Two effects are very suggestive: (i) the wings' bisector and, correspondingly, the direction of unsteady flight forces might be adapted to a given manoeuvre; (ii) the amount of flight force seems to be controlled by the extent of the approach of the wings. The situation during the fast ventral reversal seems to be even more inscrutable, since there is no idea, so far, how to estimate the direction and magnitude of the flight force produced by vortex shedding during the *quick rotation*. So far, the only suggestive comparison is that of peak rotational speeds, which would support the view of an unsteady control mechanism. However, an appropriate temporal and spatial description of the vortex shedding must be the basis of any quantitative consideration. The control system is further complicated by the temporal relationships between the force production and the instantaneous wing position; for instance, an additional force component produced during the dorsal reversal would lead to pitch-down rotations, during the ventral quick rotation to pitch-up rotations, and during the up- or downstroke to corresponding yaw turns. Few mechanisms of force production may account for a variety of control reactions determined by the specific adaptations of the geometry and timing of the wing movement. So far, these effects are prone to qualitative discussion because, at present, the deduction of the direction and magnitude of unsteady flight forces from the fine structure of kinematics is not a simple task. Future theoretical and experimental investigations might help to give a better understanding of the aerodynamic mechanisms stabilizing a small insect during flight.

I am indebted to K. G. Götz for his support throughout the study and many valuable discussions. Thanks are due to him and to A. Borst for carefully reading earlier versions of the manuscript; B. Bochenek for digitizing the films; T. Wiegand for preparing the figures; and U. Flaiz and I. Geiss for typing the manuscript. This work was supported by a grant from the M.P.G.

#### REFERENCES

- Alexander, D. D. 1986 Wind tunnel studies of turns by flying dragonflies. *J. exp. Biol.* **122**, 81–98.  
 Baker, P. S. 1979 The wing movements of flying locusts during steering behaviour. *J. comp. Physiol.* **131**, 49–58.  
 Blondeau, J. 1981 Aerodynamic capabilities of flies, as revealed by a new technique. *J. exp. Biol.* **92**, 155–163.  
 Blondeau, J. & Heisenberg, M. 1982 Three-dimensional optomotor torque system of *Drosophila melanogaster*. *J. comp. Physiol.* **145**, 321–329.  
 Collett, T. S. & Land, M. 1975 Visual control of flight behaviour in the hoverfly *Syrilla pipiens*. *J. comp. Physiol.* **99**, 1–66.

- David, C. T. 1978 The relationship between body angle and flight speed in free-flying *Drosophila*. *Physiol. Ent.* **3**, 191–195.
- David, C. T. 1985 Visual control of the partition of flight force between lift and thrust in free-flying *Drosophila*. *Nature, Lond.* **313**, 48–50.
- Dugard, J. J. 1967 Directional change in flying locusts. *J. Insect Physiol.* **13**, 1055–1063.
- Ellington, C. P. 1984*a* The aerodynamics of hovering insect flight. I. The quasi-steady analysis. *Phil. Trans. R. Soc. Lond. B* **305**, 1–15.
- Ellington, C. P. 1984*b* The aerodynamics of hovering insect flight. II. Morphological parameters. *Phil. Trans. R. Soc. Lond. B* **305**, 17–40.
- Ellington, C. P. 1984*c* The aerodynamics of hovering insect flight. III. Kinematics. *Phil. Trans. R. Soc. Lond. B* **305**, 41–78.
- Ellington, C. P. 1984*d* The aerodynamics of hovering insect flight. IV. Aerodynamic mechanisms. *Phil. Trans. R. Soc. Lond. B* **305**, 79–113.
- Ellington, C. P. 1984*e* The aerodynamics of hovering insect flight. V. A vortex theory. *Phil. Trans. R. Soc. Lond. B* **305**, 115–144.
- Ellington, C. P. 1984*f* The aerodynamics of hovering insect flight. VI. Lift and power requirements. *Phil. Trans. R. Soc. Lond. B* **305**, 145–181.
- Gettrup, E. & Wilson, D. M. 1964 The lift-control reaction of flying locusts. *J. exp. Biol.* **41**, 183–190.
- Götz, K. G. 1968 flight control in *Drosophila* by visual perception of motion. *Kybernetik* **4**, 199–208.
- Götz, K. G. 1983 Bewegungsschemen und Flugsteuerung bei der Fliege *Drosophila*. In *Biona report 2* (ed. W. Nachtigall), pp. 21–34. Stuttgart: Fischer.
- Götz, K. G. 1987*a* Course-control, metabolism and wing interference during ultralong tethered flight in *Drosophila melanogaster*. *J. exp. Biol.* **128**, 35–46.
- Götz, K. G. 1987*b* Relapse to 'preprogrammed' visual flight-control in a muscular subsystem of the *Drosophila* mutant 'small optic lobes'. *J. Neurogen.* **4**, 133–135.
- Götz, K. G. & Wandel, U. 1984 Optomotor control of the force of flight in *Drosophila* and *Musca*. II. Covariance of lift and thrust in still air. *Biol. Cybern.* **51**, 135–139.
- Götz, K. G., Hengstenberg, B. & Biesinger, R. 1979 Optomotor control of wing beat and body posture in *Drosophila*. *Biol. Cybern.* **35**, 101–112.
- Heide, G. 1983 Neural mechanisms of flight control in Diptera. In *Biona report 2* (ed. W. Nachtigall), pp. 35–52. Stuttgart: Fischer.
- Hengstenberg, R., Sandeman, D. C. & Hengstenberg, B. 1986 Compensatory head roll in the blowfly *Calliphora*. *Proc. R. Soc. Lond. B* **227**, 455–482.
- Hollick, F. S. J. 1940 The flight of the dipterous fly *Muscina stabulans* Fallén. *Phil. Trans. R. Soc. Lond. B* **230**, 357–390.
- Lighthill, M. J. 1973 On the Weis-Fogh mechanism of lift generation. *J. Fluid Mech.* **60**, 1–17.
- Maxworthy, T. 1981 The fluid dynamics of insect flight. *A. Rev. Fluid Mech.* **13**, 329–350.
- Nachtigall, W. 1966 Die Kinematik der Schlagflügelbewegungen von Dipteren. Methodische und analytische Grundlagen zur Biophysik des Insektenflugs. *Z. vergl. Physiol.* **52**, 155–211.
- Nachtigall, W. & Roth, W. 1983 Correlations between stationary measurable parameters of wing movement and aerodynamic force production in the blowfly (*Calliphora vicina* R.-D.). *J. comp. Physiol.* **150**, 251–260.
- Pfau, K. & Nachtigall, W. 1981 Der Vorderflügel großer Heuschrecken als Luftkraftezeuger. *J. comp. Physiol.* **142**, 135–140.
- Srinivasan, M. V. 1977 A visually-evoked roll response in the housefly. *J. comp. Physiol.* **119**, 1–14.
- Vogel, S. 1967 Flight in *Drosophila*. II. Variations in stroke parameters and wing contour. *J. exp. Biol.* **46**, 383–392.
- Wagner, H. 1986 Flight performance and visual control of flight of the free-flying housefly (*Musca domestica* L.) I. Organization of the flight motor. *Phil. Trans. R. Soc. Lond. B* **312**, 527–551.
- Weis-Fogh, T. 1973 Quick estimates of flight fitness in hovering animals, including novel mechanisms for lift production. *J. exp. Biol.* **59**, 169–230.
- Zalokar, M. 1947 Anatomie du thorax de *Drosophila melanogaster*. *Ref. suisse Zool.* **54**, 17–53.
- Zanker, J. M. 1988*a* How does lateral abdomen deflection contribute to flight control of *Drosophila melanogaster*? *J. comp. Physiol.* **162**, 581–588.
- Zanker, J. M. 1988*b* On the mechanism of speed- and altitude-control in *Drosophila melanogaster*. *Physiol. Entomol.* **13**, 351–361.
- Zanker, J. M. 1990 The wing beat of *Drosophila melanogaster*. I. Kinematics. *Phil. Trans. R. Soc. Lond. B* **327**, 1–18. (This volume.)
- Zanker, J. M. & Götz, K. G. 1990 The wing beat of *Drosophila melanogaster*. II. Dynamics. *Phil. Trans. R. Soc. Lond. B* **327**, 19–44. (Preceding paper.)
- Zarnack, W. 1988 The effect of forewing depressor activity on wing movement during locust flight. *Biol. Cybern.* **59**, 55–70.
- Zarnack, W. & Möhl, B. 1977 Activity of the direct downstroke flight muscles of *Locusta migratoria* (L.) during steering behaviour in flight. I. Patterns of time shift. *J. comp. Physiol.* **113**, 215–233.